# Enhancing the Frequency Adaptability of Periodic Current Controllers With a Fixed Sampling Rate for Grid-Connected Power Converters

Yongheng Yang, *Member, IEEE*, Keliang Zhou, *Senior Member, IEEE*, and Frede Blaabjerg, *Fellow, IEEE*

***Abstract*—Grid-connected power converters should employ advanced current controllers, e.g., proportional resonant (PR) and repetitive controllers (RC), in order to produce high-quality feed-in currents that are required to be synchronized with the grid voltage. The synchronization is actually to detect the instantaneous grid information (e.g., frequency and phase of the grid voltage) for the current control, which is commonly performed by a phase-locked loop (PLL) system. Hence, harmonics and deviations in the estimated frequency by the PLL could lead to current tracking performance degradation, especially for the periodic signal controllers (e.g., PR and RC) with a fixed sampling rate. In this paper, the impacts of frequency deviations induced by the PLL and/or the grid disturbances on the selected current controllers are investigated by analyzing the frequency adaptability of these current controllers. Subsequently, strategies to enhance the frequency adaptability of the current controllers are proposed for the power converters to produce high-quality feed-in currents even in the presence of grid frequency deviations. Specifically, by feeding back the PLL estimated frequency to update the center frequencies of the resonant controllers and by approximating the fractional delay using a Lagrange interpolating polynomial for the RC, respectively, the frequency-variation-immunity of these periodic current controllers with a fixed sampling rate is improved. Experiments on a single-phase grid-connected system are presented, which have verified the discussions and the effectiveness of the frequency adaptive current controllers.**

***Index Terms*—Fractional order filter, frequency adaptive, frequency variations, grid-connected power converters, Lagrange interpolating polynomial, repetitive controller, resonant controller (RES).**

## I. Introduction

POWER electronics converters have been widely used in grid-connected renewable energy systems like wind turbine systems and photovoltaic (PV) systems [1]–[3], and increasingly stringent requirements have been imposed on the grid-connected power converters [3], [4]. Due to their nonlinearity and also the intermittency, harmonic challenges are also associated with the power electronics interfaced renewable energy systems, which have to be dealt with by employing advanced control strategies according to demands [5], [6]. Commonly, a two-cascaded control system is adopted in the grid-connected power converters [7]. Since the inner current controller of the cascaded loops is responsible for shaping the current (i.e., power quality issues), great efforts have been devoted to the control of the feed-in grid current, which is also required to be synchronized with the grid voltage. Phase-locked loop (PLL) systems are widely used in the grid-connected inverters for synchronization [8]–[15]. Hence, the information (especially the grid frequency) provided by a PLL system is of importance for the current controllers, and it is extensively used at different levels of the entire control system as well as for condition monitoring [7], [16], [17]. For instance, the grid voltage phase estimated by a PLL system has been widely used for the reference frame transformation in [7]; while in [17], a PLL synchronization algorithm has been employed to detect the grid voltage fault for low-voltage ride-through operation.

In regards to the current control loop, typically, it can be implemented in the rotating reference frame ($dq$), the stationary reference frame ($\alpha\beta$), or the three-phase natural reference frame ($abc$) [7], [16], [18]. Taking the control in the $dq$-frame for an example, Park and/or Clarke transforms enable the employment of proportional-integrator (PI) controllers, where the PLL estimated grid frequency is a must for the transforms as aforementioned. Consequently, either frequency variations in the grid itself or the frequency estimation error by a PLL system will result in the control degradation when using PI controllers. On the other hand, in order to simplify the control, periodic signal controllers like repetitive controller (RC) [19]–[25] and proportional resonant (PR) controller with parallel RESonant (RES)-based harmonic compensators [7], [22], [26]–[28] are developed in either the $\alpha\beta$- or the $abc$-frame. It has been demonstrated that the periodic RES controller offers a selective harmonic control scheme, while the periodic RC compensator enables the mitigation of a wide range of harmonics [7], [16], [29]. In those cases, the control accuracy of both the PR with RES or RC controllers is inevitably affected by the designed center frequency of the resonant controller [20], [26]. Basically, the center frequency (e.g., the fundamental frequency—50 Hz) should be placed at which the control gain can approach infinite, and a constant value is selected for the sake of simplicity. As a consequence, any frequency deviation (either induced by the grid frequency changes and/or the PLL estimation errors) will inevitably lead to a finite control gain at the resonant frequencies of the periodic current controllers.

Manuscript received July 14, 2015; revised October 18, 2015 and December 7, 2015; accepted December 7, 2015. Date of publication December 10, 2015; date of current version May 20, 2016. Recommended for publication by Associate Editor C. N. M. Ho.

Y. Yang and F. Blaabjerg are with the Department of Energy Technology, Aalborg University, Aalborg 9220, Denmark (e-mail: yoy@et.aau.dk; fbl@et.aau.dk).

K. Zhou is with the Division of Systems, Power, and Energy, School of Engineering, University of Glasgow, Glasgow G12 8QQ, U.K. (e-mail: keliang.zhou@glasgow.ac.uk).

Color versions of one or more of the figures in this paper are available online at http://ieeexplore.ieee.org.

Digital Object Identifier 10.1109/TPEL.2015.2507545

In order to enhance the control performance of such periodic signal controllers, frequency adaptive schemes were developed in the prior art work [20], [21], [29]–[39]. In general, those solutions are accomplished by taking the PLL estimated frequency as a feedback of the controllers, and thus the center frequency can be updated online. For instance, in [28], the center frequencies of the RES controller are continuously adjusted according to the PLL estimated frequency. In contrast, since the RC compensator is implemented in digital controllers using $N$ unity delays ($N = f_s/f_0$ with $f_s$ and $f_0$ being the sampling and grid fundamental frequencies, respectively), the adaptive solutions are directed to ensure an integer of $N$. An intuitive possibility is to online change the sampling frequency according to the grid frequency estimated with the PLL systems [21], [34], [38]–[40], where the total cost and implementation complexity are increased, and also the stability may be challenged [39]. Moreover, this solution is suitable for the digital control systems with the multirates control capability [34], [41], or with a high precision of the controller clock [38], in such a way to update the sampling frequency online. Alternatively, properly approximating the delay number $N$ seems to be a cost-effective scheme as discussed in [20], [37], and [42], where a Lagrange-interpolating-polynomial-based filter has been used and, however, the implementation is not well addressed. Thus, this paper further investigates the above promising solution due to its cost, simplicity, portability (with less modifications), and effectiveness, especially in the digital controllers with a fixed sampling rate.

Notably, the PLL estimated frequency is essential to enhance the frequency adaptability of the periodic current controllers. However, the grid voltage as the input of the PLL systems cannot always be maintained as "constant" in terms of amplitude, frequency, and/or phase, due to multiple eventualities like continuous connection and disconnection of loads and fault to ground because of lightning strikes [43], [44]. That is why the grid codes also demand that the power converters should be able to operate within a specified frequency range or even regulate the frequency [6], [45]. Together with the background distortions in the grid voltage, a large obstacle has been posed for the PLL systems. As a result, the PLL system presents inaccuracy in the estimated frequency. Subsequently, the current controllers in the $\alpha\beta$- or the $abc$-frame will suffer from frequency deviations either due to the PLL errors or the grid disturbances [19], [20], [40], resulting in a possibility for the feed-in current to reach the total harmonic distortions (THD) limits [5], [6]. This impact is inevitable when seeing from the aforementioned, but it still lacks of a discussion on how the frequency deviation will affect the current controllers. It, thus, should be emphasized that advanced synchronizations (e.g., PLL systems) are desirable in order to ensure a reliable and satisfactory control of the grid current.

In light of the above issues, in this paper, the frequency adaptability of the selected periodic current controllers (i.e., PR, RES, and RC) is explored in the consideration of the PLL estimated frequency variations owing to either the PLL inherent errors or the grid disturbances. In Section II, a brief description of the dual-loop control method for single-phase grid-connected inverters is presented. Then, the frequency adaptability of the periodic current controllers is focused on. More important, solutions to enhance the frequency adaptability of these current controllers are discussed, being the frequency adaptive current controllers, where the implementation is also emphasized. The discussions and the effectiveness of the frequency adaptive current controllers are verified by experiments in Section IV before the conclusion.

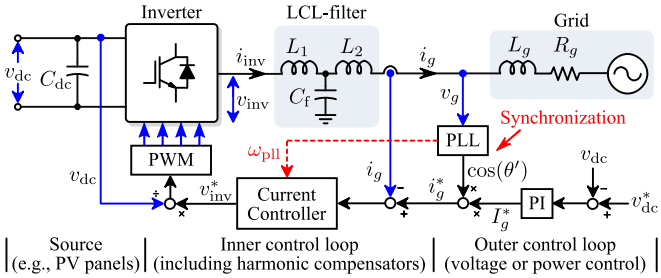


Fig. 1. Overall dual-loop control structure of a single-phase grid-connected system with an *LCL* filter and a PLL synchronization unit.

## II. Frequency Adaptability Analysis

### A. Control of Single-Phase Grid-Connected Converters

Fig. 1 shows a typical configuration of a single-phase grid-connected system and its overall cascaded dual-loop control structure, where an *LCL* filter is used considering the power quality issues [7]. It is shown in Fig. 1 that the PLL estimated grid frequency ($\omega_{\rm pll}$) is feeding back to the current controller as aforementioned in order to improve the control performance. Especially, the frequency $\omega_{\rm pll}$ is used to transform ac quantities (i.e., the grid current $i_g$ and voltage $v_g$) to dc quantities (i.e., $\mathbf{i}_{\rm dq}$ and $\mathbf{v}_{\rm dq}$) for PI controllers in the $dq$-frame or reversely ($dq \rightarrow \alpha\beta$). Yet for simplicity, in the case of the current control in either the $\alpha\beta$- or the $abc$-frame, a fixed constant frequency (i.e., the nominal grid frequency $\omega_0$) is designed for the periodic current harmonic controllers in practice (especially, when implemented in a digital signal processor), as it is shown in Fig. 2. In both cases, the current controller performance will be affected by the PLL estimated frequency, which is used to generate the grid current reference according to Fig. 1. Notably, other current controllers like the deadbeat (DB) control can also be used as the fundamental-frequency current controller [46], [47].

### B. Frequency Sensitivity Analysis of the Current Controllers

In practice, it is difficult to attain an acceptable feed-in current even with high-order grid filters (e.g., an *LCL* filter) because of the always existing background distortions in the grid voltage. Moreover, the grid-side filter should be cost- and size-effective in commercial applications, e.g., using an *LC* filter. Thus, harmonic compensators are typically incorporated in the current control loop in order to improve the current quality, as it is shown in Fig. 2, where the fundamental-frequency current controller (i.e., $G_{\rm PR}(s)$) can be given as

$$G_{\rm PR}(s) = k_p + \frac{k_i s}{s^2 + \omega_0^2} \tag{1}$$

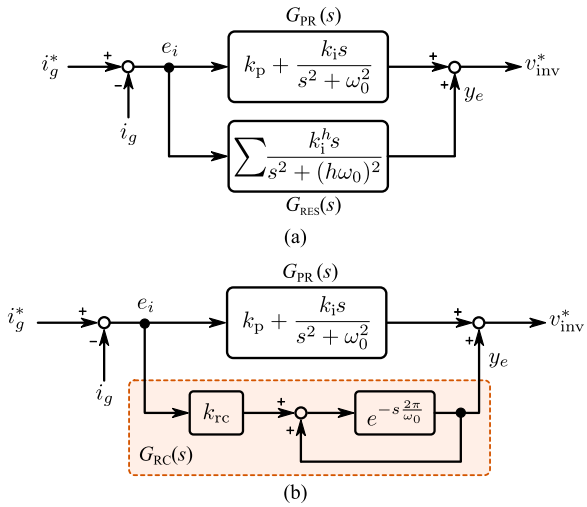


Fig. 2. PR current controller $G_{\mathrm{PR}}(s)$ with (a) resonant harmonic controller $G_{\mathrm{RES}}(s)$ and (b) repetitive harmonic compensator $G_{\mathrm{RC}}(s)$.

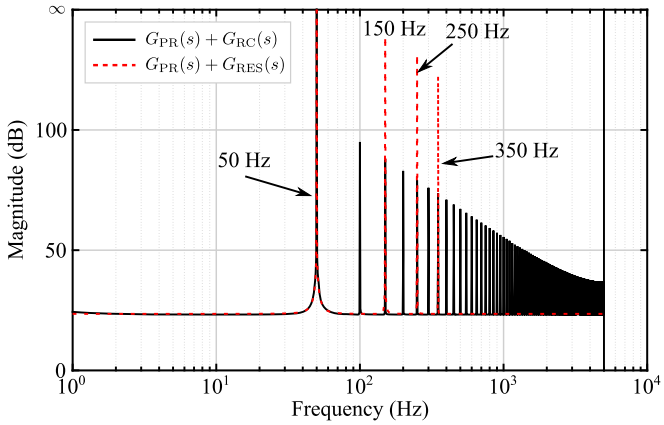


Fig. 3. Magnitude response of the current controllers shown in Fig. 2, where $h = 3, 5, 7$.

in which $k_p$ and $k_i$ are the control gains. It can be seen in Fig. 2 that the harmonic compensator embraces either a paralleled multiresonant controller $G_{\mathrm{RES}}(s)$ or an RC $G_{\mathrm{RC}}(s)$, which exhibits good performance for controlling periodic signals (i.e., the grid current $i_g$) [7], [16], [20], [22]. Accordingly, the harmonic compensators can be expressed as

$$G_{\mathrm{RES}}(s) = \sum_{h=3,5,7,\ldots} G_{\mathrm{RES}}^{h}(s) \tag{2}$$

$$G_{\mathrm{RC}}(s) = \frac{k_{\mathrm{rc}} e^{-2\pi s/\omega_0}}{1 - e^{-2\pi s/\omega_0}} \tag{3}$$

where $G_{\mathrm{RES}}^{h}(s)$ is the $h$th-order resonant controller with $h$ being the harmonic order and $k_{\mathrm{rc}}$ is the control gain of the RC harmonic compensator. Furthermore, the individual resonant controller can be given as

$$G_{\mathrm{RES}}^{h}(s) = \frac{k_i^h s}{s^2 + (h\omega_0)^2} \tag{4}$$

in which $k_i^h$ is the control gain of the corresponding $h^{\mathrm{th}}$-order resonant controller. In addition, the RC-based harmonic controller can further be expanded into [47]

$$G_{\mathrm{RC}}(s) = k_{\mathrm{rc}}\left[-\frac{1}{2} + \frac{\omega_0}{2\pi s} + \frac{\omega_0}{\pi}\sum_{k}\frac{s}{s^2 + (k\omega_0)^2}\right] \tag{5}$$

with $k = 1, 2, 3, \ldots$. Equation (5) indicates the inherent resonant characteristic of the RC controller with an identical resonant gain (i.e., $k_{\mathrm{rc}}\omega_0/\pi$), and it also shows that the internal models of the dc signal and all harmonics are incorporated in the harmonic compensator $G_{\mathrm{RC}}(s)$.

According to Fig. 2, the error rejection transfer function $G_e(s)$ can be given as

$$G_e(s) = \frac{E_i(s)}{I_g^*(s)} = \frac{1}{1 + [G_{\mathrm{CC}}(s) + G_{\mathrm{HC}}(s)]\,G_p(s)} \tag{6}$$

with $G_{\mathrm{CC}}(s)$ being the fundamental-frequency current controller (e.g., PR or DB controllers), $G_{\mathrm{HC}}(s)$ being the harmonic compensators (e.g., RES or RC controllers), and $G_p(s)$ being the plant model. When $s \to jk\omega_0$, it can be seen from (1)–(5) that the magnitude response of these controllers will theoretically approach to infinite (i.e., $|G_{\mathrm{CC}}(jk\omega_0) + G_{\mathrm{HC}}(jk\omega_0)| \to \infty$), as illustrated in Fig. 3. Consequently, the tracking error $e_i(t)$ ($E_i(s)$ in (6)) will be zero at the frequencies of interest (i.e., $k\omega_0$). In other words, the RES controller enables a selective harmonic compensation, while the RC controller can eliminate all harmonics below the Nyquist frequency theoretically, being a good alternative for harmonic control [20]–[22], [48].

However, in practical applications, the grid frequency is not exactly the nominal one $\omega_0$, but a time-varying element of the grid voltage with small deviations. Hence, in most grid standards [43], [44], it is also demanded that the grid-connected devices should be able to operate within a certain frequency range. Under short-term abnormal grid conditions (e.g., a frequency sag), the inverter-based systems are even required to ride through such events [6], [49]. Nonetheless, in those cases, infinite magnitudes of those current controllers cannot always be maintained when $s \to jk\omega_{\mathrm{pll}}$, leading to reduced tracking performance and thus a poor THD of the feed-in current. Even with an advanced PLL system, the frequency deviations cannot be completely eliminated. In general, the PLL estimated frequency $\omega_{\mathrm{pll}}$ can be expressed as

$$\omega_{\mathrm{pll}} = \omega_0 + \Delta\omega \tag{7}$$

in which $\Delta\omega = \Delta\omega_g + \Delta\omega_{\mathrm{pll}}$ represents the estimated angular frequency deviations. It consists of the grid frequency disturbances $\Delta\omega_g = \omega_g - \omega_0$ with $\omega_g$ being the instantaneous grid frequency and/or the PLL tracking errors $\Delta\omega_{\mathrm{pll}}$. As discussed above, (1)–(5) and (7) imply that a small frequency variation (i.e., $\Delta\omega$) induced by the grid frequency changes and/or PLL estimation errors can contribute to a degradation of the error rejection capability for those current controllers, which are supposed to approach to infinite at the targeted frequencies (i.e., $k\omega_{\mathrm{pll}}$). This impact is referred to as the frequency adaptability, which is illustrated as the following.

According to (4) and (7), the magnitude response (i.e., $s = jh\omega_{\mathrm{pll}}$) of an individual resonant controller $G_{\mathrm{RES}}^{h}(s)$ at the

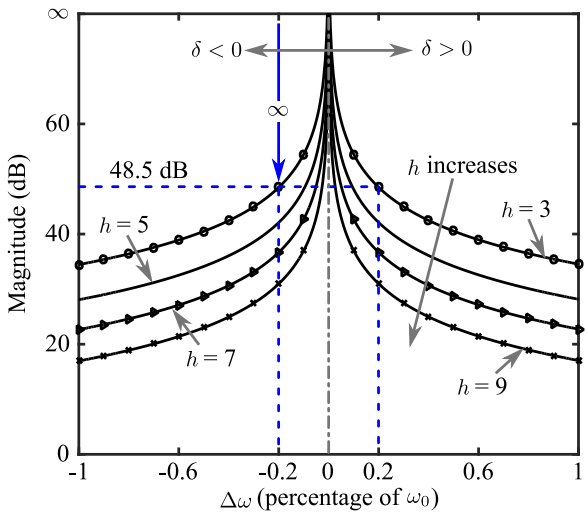


Fig. 4. Magnitudes of the resonant controller $G^h_{\rm RES}(s)$ as a function of the frequency variation $\Delta\omega$ with $k_i^3 = 1000$, $k_i^5 = 800$, $k_i^7 = 600$, and $k_i^9 = 400$.

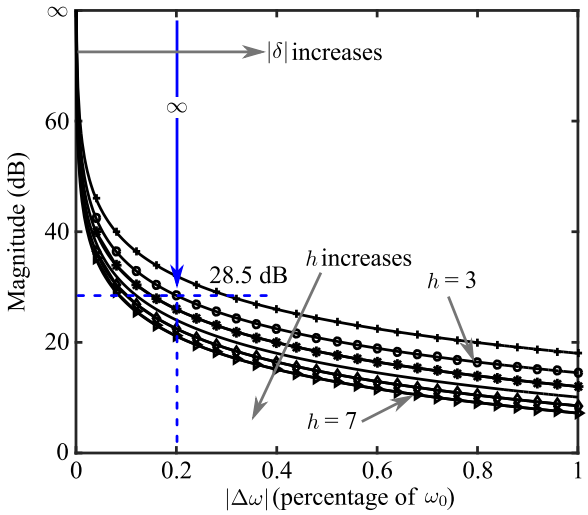


Fig. 5. Magnitudes of the RC $G_{\rm RC}(s)$ as a function of the frequency variation $\Delta\omega$, where $k_{\rm rc} = 1$.

corresponding frequency ($h\omega_{\rm pll}$) can be obtained as

$$\left|G^h_{\rm RES}\left(jh\omega_{\rm pll}\right)\right| = \left|\frac{jk_i^h h\omega_{\rm pll}}{-h^2\omega_{\rm pll}^2 + h^2\omega_0^2}\right| = \frac{k_i^h}{h\omega_0}\left|\frac{\delta+1}{\delta^2+2\delta}\right| \tag{8}$$

with $\delta = \Delta\omega/\omega_0$, and (8) indicates that the gain will not be infinite unless $\delta = 0$ (i.e., $\Delta\omega = 0$). The control gain reduction of the resonant controllers due to the frequency variations $\Delta\omega$ is illustrated in Fig. 4, where it can be observed that even a small frequency variation of $\pm 0.2\%$ can result in a significant performance degradation of the resonant controllers (e.g., the magnitude decreases from $\infty$ dB to 48.5 dB). It demonstrates that the RES-based harmonic compensator (and also the resonant controller of the PR controller with $h = 1$) is sensitive to frequency variations. In other words, the RES controller in (4) has a poor frequency-variation-immunity.

In the same manner, substituting $s = jh\omega_{\rm pll}$ into (3) gives the magnitude response of the RC controller $G_{\rm RC}$ as

$$\left|G_{\rm RC}\left(jh\omega_{\rm pll}\right)\right| = \left|\frac{k_{\rm rc}e^{-j\cdot 2\pi h(1+\delta)}}{1-e^{-j\cdot 2\pi h(1+\delta)}}\right|. \tag{9}$$

According to Euler's formula, the following is obtained:

$$\left|G_{\rm RC}\left(jh\omega_{\rm pll}\right)\right| = \frac{k_{\rm rc}}{\sqrt{2-2\cos\left(2\pi h\delta\right)}} \tag{10}$$

which implies that the RC controller no longer can approach infinite control gain when there is a frequency tracking error from the PLL system (and/or grid frequency changes), i.e., $\delta \neq 0$ and $\Delta\omega \neq 0$. Fig. 5 further illustrates the effect of a frequency deviation on the current control error rejection ability of the RC harmonic compensator. As it can be observed in Fig. 5, a remarkable gain drop (e.g., the magnitude decreases from $\infty$ to 28.5 dB) occurs due to a frequency change of $\pm 0.2\%$ (i.e., corresponding to a frequency variation of $\pm 0.1$ Hz in 50-Hz systems), and consequently the rejection ability is significantly degraded. A conclusion drawn from Figs. 4 and 5 is that the frequency sensitivity of the periodic current controllers (i.e., the PR, RES, and RC controllers) is poor, and thus enhancing the frequency adaptability is necessary in order to produce high-quality currents.

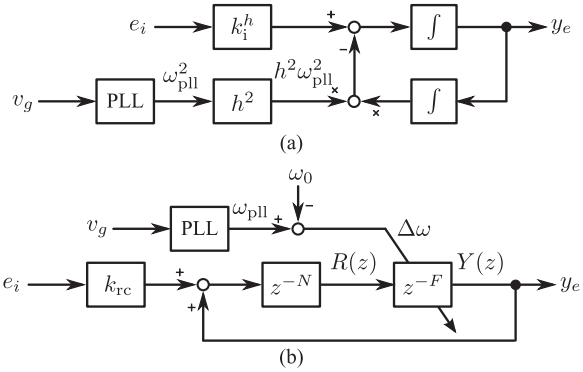


Fig. 6. Frequency-variation-immunity enhanced periodic current harmonic compensators: (a) resonant controllers and (b) RC.

## III. Enhancing the Frequency Adaptability

As discussed in the last paragraph, in order to achieve a good current control in terms of a zero-error elimination of the harmonics even under a variable grid frequency (or a PLL tracking error), the current controllers have to be frequency adaptive. It means that the control gain should be infinite when $s = jh\omega_{\rm pll}$. Thus, feeding back the frequency estimated by an advanced PLL system [10] or frequency estimator (e.g., using Kalman filter) [13], [14] to the current controllers is a possibility to decrease the frequency sensitivity. This is much convenient for the resonant controllers [30], [31], [35], which is given as

$$G^h_{\rm RES}(s) = \frac{k_i^h s}{s^2 + (h\omega_{\rm pll})^2} = \frac{k_i^h s}{s^2 + \left[h(\omega_0 + \Delta\omega)\right]^2}. \tag{11}$$

Fig. 6(a) shows the implementation of a frequency adaptive resonant controller. It can be observed in Fig. 6(a) and (11) that by feeding in the PLL estimated frequency, the resonant frequencies of the harmonic controllers $G^h_{\rm RES}(s)$ will automatically be

TABLE I
COEFFICIENTS OF THE LAGRANGE-INTERPOLATING-POLYNOMIAL-BASED FRACTIONAL DELAY FILTER $z^{-F}$ WITH $F$ BEING THE FILTER ORDER

| $H_l$ | $L=1$ (Linear) | $L=3$ (Cubic) |
|---|---|---|
| $H_0$ | $1-F$ | $-(F-1)(F-2)(F-3)/6$ |
| $H_1$ | $F$ | $F(F-2)(F-3)/2$ |
| $H_2$ | | $-F(F-1)(F-3)/2$ |
| $H_3$ | | $F(F-1)(F-2)/6$ |

adjusted to the instantaneously estimated grid frequency. As a result, infinite gains of the resonant controllers are almost attained in the case of a varying grid frequency.

However, in respect to the RC controller, enhancing the frequency adaptability cannot be reached by simply feeding back the PLL estimated frequency, since the RC controller is normally implemented in a digital signal processor of a fixed sampling rate. In that case, the RC controller shown in (3) can be given as

$$G_{\mathrm{RC}}(z)=\frac{k_{\mathrm{rc}}z^{-(N+F)}}{1-z^{-(N+F)}} \tag{12}$$

in which $N=\lfloor f_s/f \rfloor$ is an integer, $F=f_s/f-N$ is the order of a fractional delay (i.e., $z^{-F}$) with $f=\omega_{\mathrm{pll}}/(2\pi)$, and $f_s$ is the sampling frequency. Therefore, to enhance the frequency adaptability of the RC controller, one possibility is that the fractional delay $z^{-F}$ induced by the frequency variations, which is neglected in practice, should be appropriately approximated. A cost-effective approach to approximate the fractional delay is using finite-impulse response (FIR) filters as discussed in [20], [37], [42], and [50]. It should be noted that the frequency adaptability of the RC harmonic compensator can be enhanced alternatively by varying the sampling frequency [21], [34], which in return is able to ensure an integer of $f_s/f$ (i.e., $F=0$) in practical applications, but it will increase the cost and the overall complexity. Such enhancement of the frequency adaptability by varying the sampling frequency is impossible (or difficult) to implement in the case of a control system with a fixed sampling rate (e.g., a dSPACE DS1103 system). Furthermore, the adaptive scheme requires major modifications (reprogramming) when the control algorithm is transferred to another system, i.e., poor portability, in contrast to the frequency adaptive solutions based on digital filters.

The most popular but simple and effective solution to the FIR fractional delay $z^{-F}$ is based on the Lagrange interpolating polynomial, which can be expressed as

$$z^{-F}\approx\sum_{l=0}^{L}\left(z^{-l}H_l\right)\ \text{with}\ H_l=\prod_{\substack{i=0\\ i\neq l}}^{L}\frac{F-i}{l-i} \tag{13}$$

where $H_l$ is the Lagrange interpolating polynomial coefficient $l, i=0, 1, 2, \ldots, L$, and $L$ is the length of the Lagrange-interpolation-based fractional delay filter. For convenience, the coefficients of the Lagrange-based fractional delay filter $z^{-F}$ are given in Table I. If $L=1$, (13) corresponds to a linear interpolation between two samples, i.e., $z^{-F}\approx H_0+H_1z^{-1}$. While in the case of $L=3$, a cubic interpolating polynomial

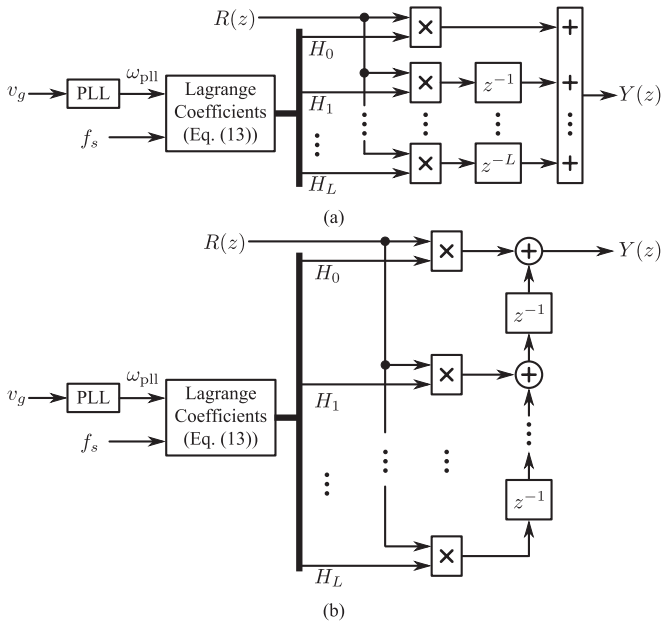


Fig. 7. Different implementations of the fractional delay filter, where $z^{-F}=Y(z)/R(z)$: (a) parallel structure [20] and (b) Farrow structure [50].

is formulated, i.e., $z^{-F}\approx H_0+H_1z^{-1}+H_2z^{-2}+H_3z^{-3}$, which has been proved in [20], [42], [47], and [50] as a relatively good and accurate approximation of the fractional delay $z^{-F}$ in terms of the bandwidth and also the resultant phase delay. As a consequence, the Lagrange-based FIR filter with $L=3$ can be employed to enhance the frequency-variation-immunity of the RC compensator. Following, the general block diagram of a frequency adaptive RC harmonic compensator can be constructed as shown in Fig. 6(b).

Although the Lagrange-interpolation-polynomial-based fraction delay filter has several advantages like easy formulas for the coefficients and good response at low frequencies [50], it may still consume certain memory space if not efficiently implemented in the digital control systems. Moreover, when comparing the frequency adaptive schemes for the RES and RC controllers in Fig. 6, the frequency delay order $F$ has an indirect mapping relationship with the frequency variations $\Delta\omega$, requiring an online calculation of the Lagrange coefficients according to the PLL estimated angular frequency $\omega_{\mathrm{pll}}$ and the system sampling frequency $f_s$, which is a fixed value in this case.

Fig. 7 gives two possibilities to implement digitally the fractional delay filter of (13) in low-cost digital signal processors. It can be observed that the Farrow structure [50] has less delay units and thus consumes less memory space compared to the direct structure that has been employed in [20]. Thus, the Farrow structure is a more efficient implementation of the fractional delay filter. Table II further summaries the computational burden (complexity) of the two fractional delay filter structures. It can be seen that, in terms of implementation, the frequency adaptive scheme for the RC harmonic compensator is more complicated than that for the RES controller. However, when compensating high-order harmonics is required, the memory consumed by the RES controller is increased, which is not the case for the RC

TABLE II
COMPLEXITY COMPARISON OF THE FRACTIONAL DELAY FILTER IMPLEMENTATIONS (SEE FIG. 7)

| | Parallel structure | Farrow structure |
|---|---|---|
| No. of summations | $L$ | $L$ |
| No. of multiplications | $L+1$ | $L+1$ |
| No. of delays | $L(L+1)/2$ | $L$ |
| Structure type | In parallel | Series connection |

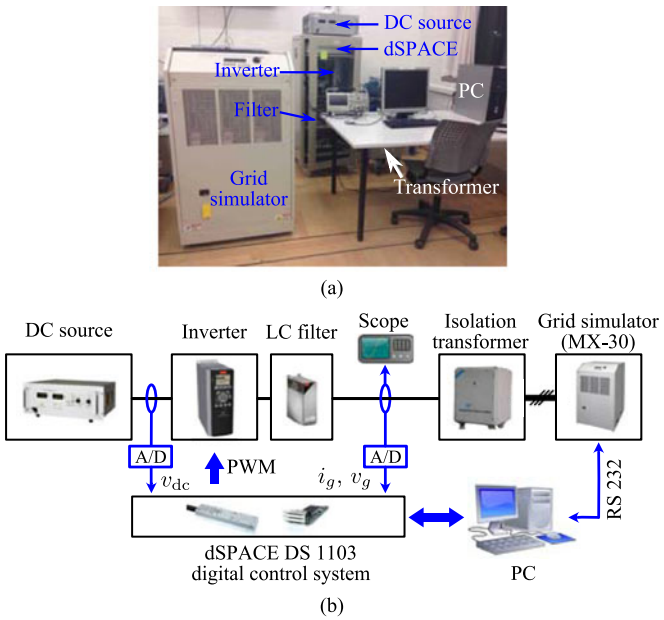


Fig. 8. Experimental setup of a single-phase grid-connected inverter system: (a) test-rig photo and (b) implementation block diagrams.

compensator [24]. Nevertheless, the above discussions have revealed that an advanced PLL system in terms of accuracy and dynamics is crucial for the enhancement of the controller frequency adaptability, especially for single-phase grid-interfaced converters, as discussed in the beginning of Section III.

## IV. EXPERIMENTAL VERIFICATIONS

### A. Test-Rig Description

In order to verify the above analysis and also to test the effectiveness of the enhanced frequency adaptability of the current controllers, experiments have been carried out on a single-phase grid-connected inverter system, where an ac programmable power source has been used in order to change the frequency. Fig. 8 shows the experimental setup, where a commercial inverter is adopted and an *LC* filter is used. The voltage of the capacitor $C_f$ is measured for synchronization. The other system parameters are listed in Table III. For comparison, a DB controller and the PR controller are adopted as the fundamental-frequency current controller, and the RES and RC controllers are used to compensate the harmonics. As for the synchronization, a second-order-generalized integrator-based PLL (SOGI-PLL) algorithm [7], [8] has been adopted due to its robust immunity to background distortions and fast dynamics. Fig. 9 shows the

TABLE III
PARAMETERS OF THE SINGLE-PHASE GRID-CONNECTED SYSTEM SHOWN IN FIG. 8

| Parameter | Symbol | Value |
|---|---|---|
| Nominal grid voltage amplitude | $v_{gn}$ | 311 V |
| Nominal grid frequency | $\omega_0$ | $2\pi\times50$ rad/s |
| Rated power | $P_n$ | 1 kW |
| DC-link voltage | $v_{dc}$ | 400 V |
| DC-link capacitor | $C_{dc}$ | 1100 $\mu$F |
| Grid impedance | $L_g$ | 2 mH |
| | $R_g$ | 0.2 $\Omega$ |
| *LC* filter | $L_1$ | 3.6 mH |
| | $C_f$ | 2.35 $\mu$F |
| Switching and sampling frequencies | $f_{sw}$, $f_s$ | 10 kHz |

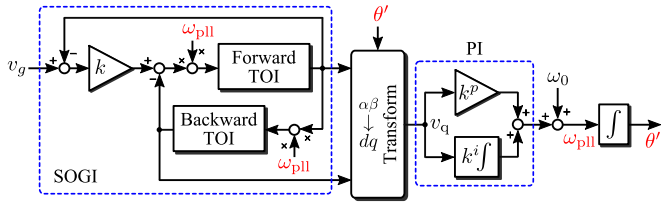


Fig. 9. Digital implementation (structure) of the SOGI-PLL system.

structure of the SOGI-PLL system, in which two third-order integrators (TOI) [8] have been employed to realize the SOGI system, with $k$ being the control gain for the SOGI in-quadrature structure, and $k^p$, $k^i$ being the proportional and integral control gains for the PI controller (i.e., the PLL loop filter), respectively. In this paper, $k=1.4$, $k^p=0.283$, and $k^i=5.663$, which will result in an optimal performance of the SOGI-PLL system in terms of overshoot and settling time [8], [16].

### B. Discrete Current Controllers

Since the control systems were done in a dSPACE DS 1103 system, the resonant controller can easily be implemented in a discrete form using one Forward Euler method and one Backward Euler method [8], [35]. Then, the frequency adaptive RES harmonic compensator can be obtained in its discrete form as

$$G^h_{\mathrm{RES}}(z)=\frac{k^h_i(z^{-1}-z^{-2})T_s}{1+(h^2\omega^2_{\mathrm{pll}}T^2_s-2)z^{-1}+z^{-2}} \tag{14}$$

with $T_s=1/f_s$ being the sampling period. Notably, other discretization methods like the Tustin with prewarping, the impulse invariant, and the Trapezoidal method can be employed to discretize the resonant controller of (4) at the cost of increased complexity [8]. While for the DB controller [16], it can be expressed as

$$G_{\mathrm{DB}}(z)=\frac{z^{-1}}{(1-z^{-1})G_f(z)} \tag{15}$$

where $G_f(z)$ is the filter model. In practice, a low-pass filter is incorporated into the RC controller in order to improve the controller robustness [47]. Then, the RC harmonic compensator of (3) is modified as given by

$$G_{\mathrm{RC}}(z)=\frac{k_{\mathrm{rc}}z^{-(N+F)}Q(z)}{1-z^{-(N+F)}Q(z)}\cdot C(z) \tag{16}$$

TABLE IV
PARAMETERS OF THE CURRENT CONTROLLERS/COMPENSATORS

| Controller | Symbol | Value |
|---|---|---|
| PR controller | $k_p$, $k_i$ | 22, 2000 |
| Resonant controller (RES) | $k_i^3$, $k_i^5$, $k_i^7$ | 1000 |
| Repetitive controller (RC) | $k_{\rm rc}$ | 1.8 |
| Low pass filter $Q(z)$ | $\alpha_0$, $\alpha_1$ | 0.8, 0.1 |
| Phase-lead compensator $C(z)$ | $m$ | 3 |

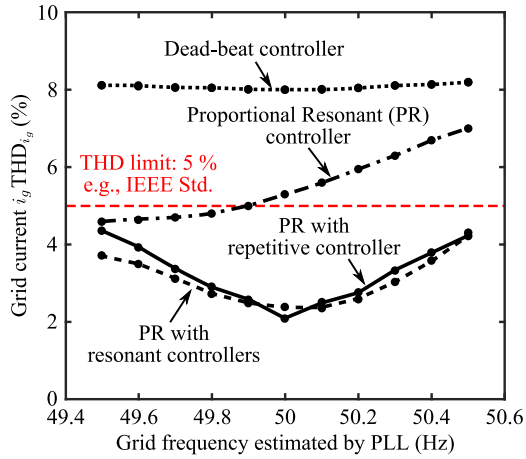


Fig. 10. Experimental verification of the frequency adaptability of the DB and PR fundamental-frequency current controllers, and the resonant and repetitive based harmonic controllers under a constant loading condition (i.e., $I_g^* = 5$ A).

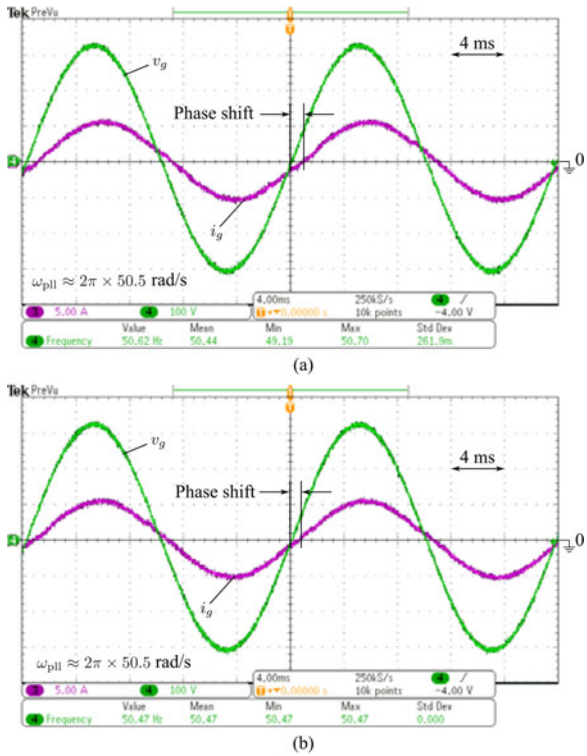


Fig. 11. Steady-state performance of the PR controller with harmonic compensators ($I_g^* = 5$ A, CH3—grid current $i_g$ [5 A/div]; CH4—grid voltage $v_g$ [100 V/div]): (a) resonant controllers and (b) RC, where the grid frequency is 50.5 Hz.

in which $Q(z) = \alpha_1 z + \alpha_0 + \alpha_1 z^{-1}$ is the low-pass filter with $\alpha_0 + 2\alpha_1 = 1$ and $\alpha_0, \alpha_1 > 0$, and $C(z) = z^m$ is a phase-lead compensator. The phase-lead number $m$ of $C(z)$ is practically determined in the experimental tests. All the parameters of these controllers are shown in Table IV, where it can be seen that only the third, fifth, and seventh RES controllers were incorporated with the fundamental-frequency controller (i.e., the PR controller) for harmonic compensation.

### C. Experimental Results—Constant Loading

The frequency adaptability of the discussed current controllers in the case of a varying grid frequency has first been tested, when a constant loading condition (i.e., reference current amplitude $I_g^* = 5$ A) is considered. The test results are shown in Fig. 10, in which the grid frequency was programmed within a range of 49.5 to 50.5 Hz (i.e., $\pm 1\%$). It can be observed in Fig. 10 that the DB controller is almost immune to frequency deviations due to its model-dependent characteristic with a relatively low demand of the grid frequency information [46], [51]. In fact, the DB current controller behaves like a simple proportional controller according to (15), and hence, its harmonic rejection capability is also poor. In contrast, the PR current controller is significantly affected by the grid frequency changes. Specifically, when the grid frequency increases, the performance of the PR controller is significantly degraded, thus resulting in a poor current THD that may exceed the limitation (e.g., THD $< 5\%$) [5]. However, due to the inverter nonlinearity and/or deadtime effect [52], which induces low-order harmonics, the harmonic compensators (e.g., RES and RC compensators) should be included in parallel with the two fundamental current controllers (i.e., DB and PR controllers) in order to improve the current quality. Nevertheless, those harmonic compensators may also be affected by the frequency variations. For instance, as it is shown in Fig. 10, both the RES and the RC periodic current controllers present poor frequency adaptability, since they are highly frequency-dependent controllers (i.e., their realizations rely on the grid frequency information provided by a PLL system or a frequency estimator). The test results are in a close agreement with the analysis presented in Section II.B (see Fig. 4).

Moreover, the poor frequency adaptability is further verified by the steady-state performance of the RES and RC controllers under a severe abnormal grid frequency (i.e., $2\pi \times 50.5$ rad/s), as it is shown in Fig. 11. Although the control objective is to feed-in a high-quality current at unity power factor, it, however, can be observed in Fig. 11 that there is a phase shift between the grid voltage $v_g$ and the feed-in grid current $i_g$ due to the frequency deviation, and thus leading to a poor power factor. That is to say, the grid-connected inverter system is not operating at unity power factor mode, which may violate the integration demands. Nevertheless, the above experimental results have demonstrated the frequency-variation-immunity of the selected current controllers, i.e., the DB and PR fundamental-frequency current controllers, and the RES and RC harmonic compensators.

According to the discussions in Section III, the strategies to enhance the frequency adaptability of the periodic current controllers were applied and the single-phase grid-connected

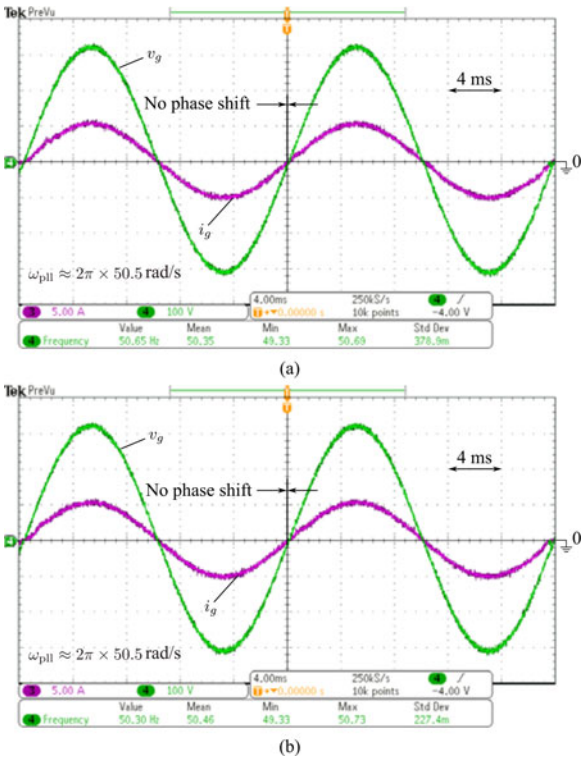


Fig. 12. Steady-state performance of the frequency adaptive current controllers ($I_g^* = 5$ A, CH3—grid current $i_g$ [5 A/div]; CH4—grid voltage $v_g$ [100 V/div]): (a) resonant controllers and (b) RC, where the grid frequency is 50.5 Hz and a frequency adaptive PR controller is employed as the fundamental-frequency current controller.

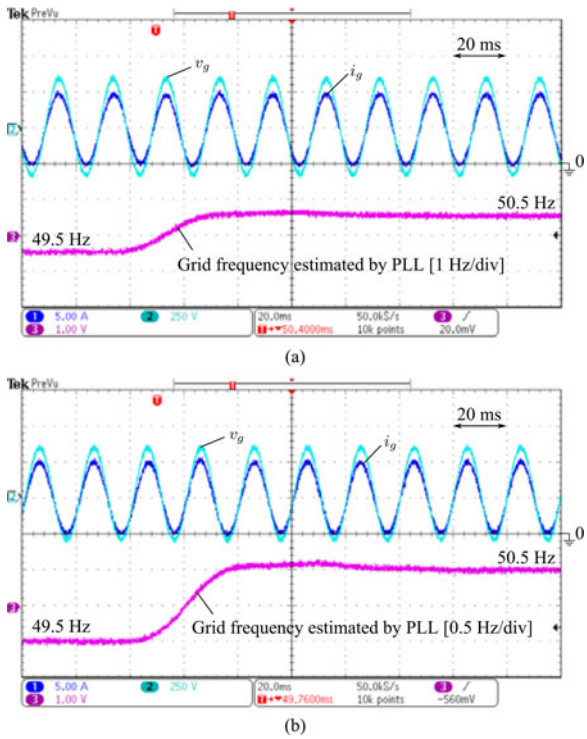


Fig. 13. Dynamic performance of the frequency adaptive PR controller with harmonic compensators (CH1—grid current $i_g$ [5 A/div]; CH2—grid voltage $v_g$ [100 V/div]; CH3—PLL output frequency): (a) frequency adaptive resonant controllers and (b) frequency adaptive repetitive compensator, where the grid frequency changed from 49.5 to 50.5 Hz under a constant loading condition (i.e., $I_g^* = 5$ A).

inverter system has been tested. Fig. 12 shows the steady-state performances of the enhanced periodic current controllers. It can be observed in Fig. 12(a) that when the PLL estimated frequency $\omega_{\rm pll}$ is fed back to the resonant controller of (14), the tracking performance is improved. As a result, in the case of frequency variations induced by the grid disturbances, a unity power factor operation as well as an improved current quality is always achieved. Similarly, when applying the frequency adaptive scheme to the RC harmonic compensator, there is no phase shift between the grid voltage and the injected grid current as shown in Fig. 12(b), and i.e., the system is operating at a unity power factor to feed in high-quality currents. It should be pointed out that the parallel structure shown in Fig. 7(a) has been adopted for adapting the RC harmonic compensator to grid frequency changes without considering the implementation efficiency.

In addition, the dynamics of the frequency adaptive schemes were tested in the case of a grid-frequency step-up change (i.e., from 49.5 to 50.5 Hz). The experimental results are presented in Fig. 13, which has verified the effectiveness of the proposed frequency adaptive schemes in terms of dynamics. Similar conclusion can be drawn: it is convenient to feed back the PLL estimated frequency according to Fig. 6(a) in such a way that the frequency adaptability of the RES controller is effectively improved; while by approximating the fractional order delay according to Fig. 7(a), the frequency adaptability of the RC harmonic controller is also enhanced. Both will contribute to an

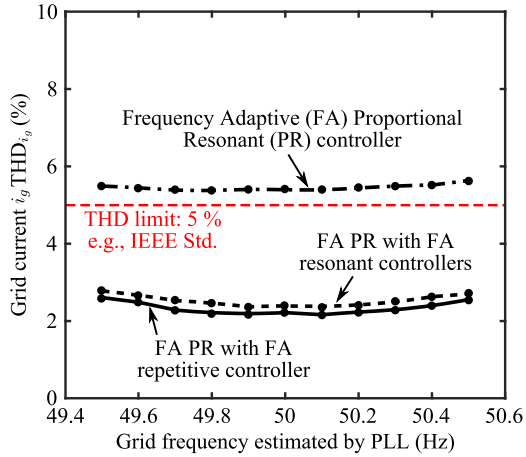


Fig. 14. Performance (experiments) of the PR controller with and w/o harmonic compensators (i.e., resonant controllers or the RC) under a constant loading condition (i.e., $I_g^* = 5$ A), where the frequency-variation-immunity is enhanced according to Figs. 6 and 7.

improved power factor as well as a lower THD of the feed-in currents.

Fig. 14 has further validated the effectiveness of the discussed adaptive schemes to enhance the frequency-variation-immunity of the selected current controllers under a wide range of grid frequency variations (i.e., 49.5–50.5 Hz). When compared with the THD$_{i_g}$ shown in Fig. 10, it can be observed in Fig. 14 that the periodic current controllers with the frequency adaptability

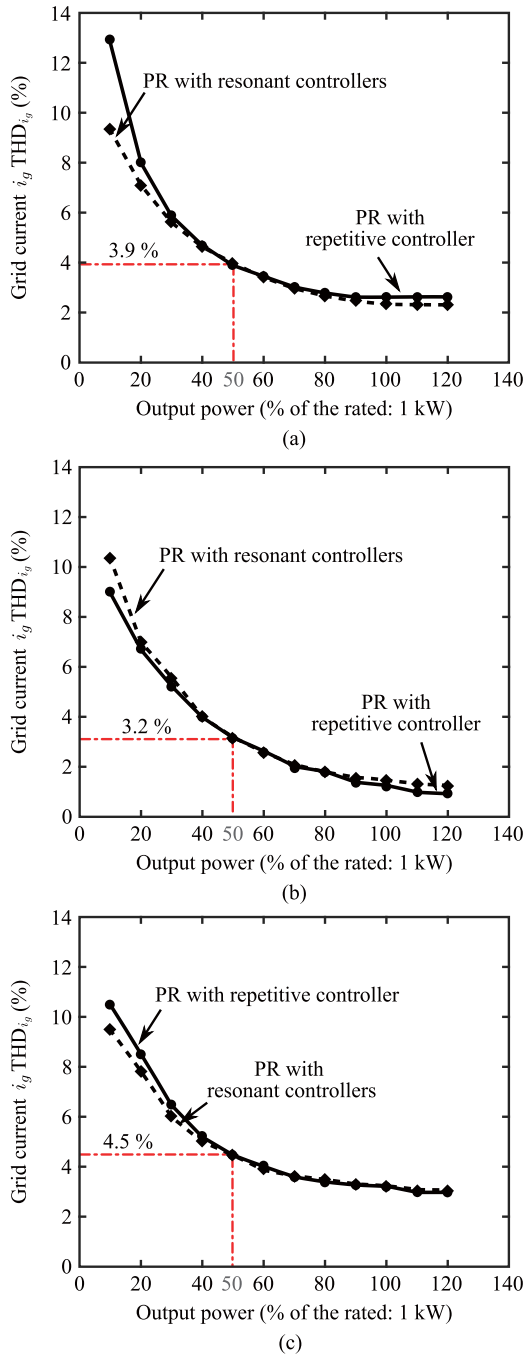


Fig. 15. Performance (experiments) of the PR controller without enhanced frequency adaptability under different power loading, where the resonant and the RCs are adopted for harmonic compensation and the grid frequency is: (a) 49.5 Hz, (b) 50 Hz, and (c) 50.5 Hz.

schemes in Section III can maintain an almost constant THD despite the variations of the grid frequency with a robust PLL system for the frequency estimation. It is also worth to point out that the RC harmonic controller consists of all the resonant controllers with the corresponding frequency below the Nyquist frequency. As a consequence, for the PR controller with an RC as the harmonic compensator, the grid current THD is lower than that in the case when the resonant controllers are paralleled as the harmonic compensator, where only a number of harmonics are selectively compensated.

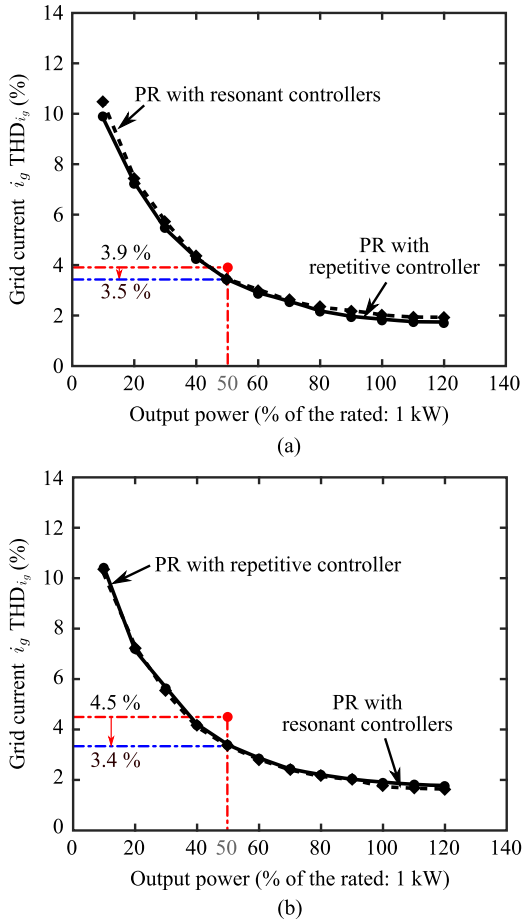


Fig. 16. Performance (experiments) of the PR (frequency adaptive) controller with enhanced frequency adaptability under different power loading, where the frequency adaptive resonant and the frequency adaptive RCs are adopted for harmonic compensation and the grid frequency is: (a) 49.5 Hz and (b) 50.5 Hz.

### *D. Experimental Results—Various Loading*

Additionally, partial loading operations of the single-phase grid-connected inverter system have been conducted, where an extra inductor of 3.6 mH is connected between the *LC* filter and the isolation transformer. In this sense, a weak grid is to some extent simulated (i.e., the grid impedance is large, consisting of the leakage inductance of the transformer and the extra inductor), which may challenge the stability of the entire system [53]. Noted that the voltage across the filter capacitor $C_f$ is still measured for synchronization like the previous case. All other parameters are listed in Table III. Fig. 15 shows the performance of the selected periodic current controllers under different grid frequencies. It has been observed that in the case of an abnormal grid frequency, the feed-in current is getting worse with a lower THD$_{i_g}$, as illustrated previously. For instance, under the half-loading condition, the THD$_{i_g}$ has been drifted to around 3.9% (49.5 Hz) and 4.5% (50.5 Hz) from 3.2% (50 Hz), when either the RES controller or the RC compensator is used for harmonic compensation. Those test results further illustrate the poor frequency adaptability of the selected periodic current harmonic controllers (i.e., the RES and RC controllers).

Hereafter, the frequency adaptive schemes are applied to these periodic current controllers, and the same single-phase

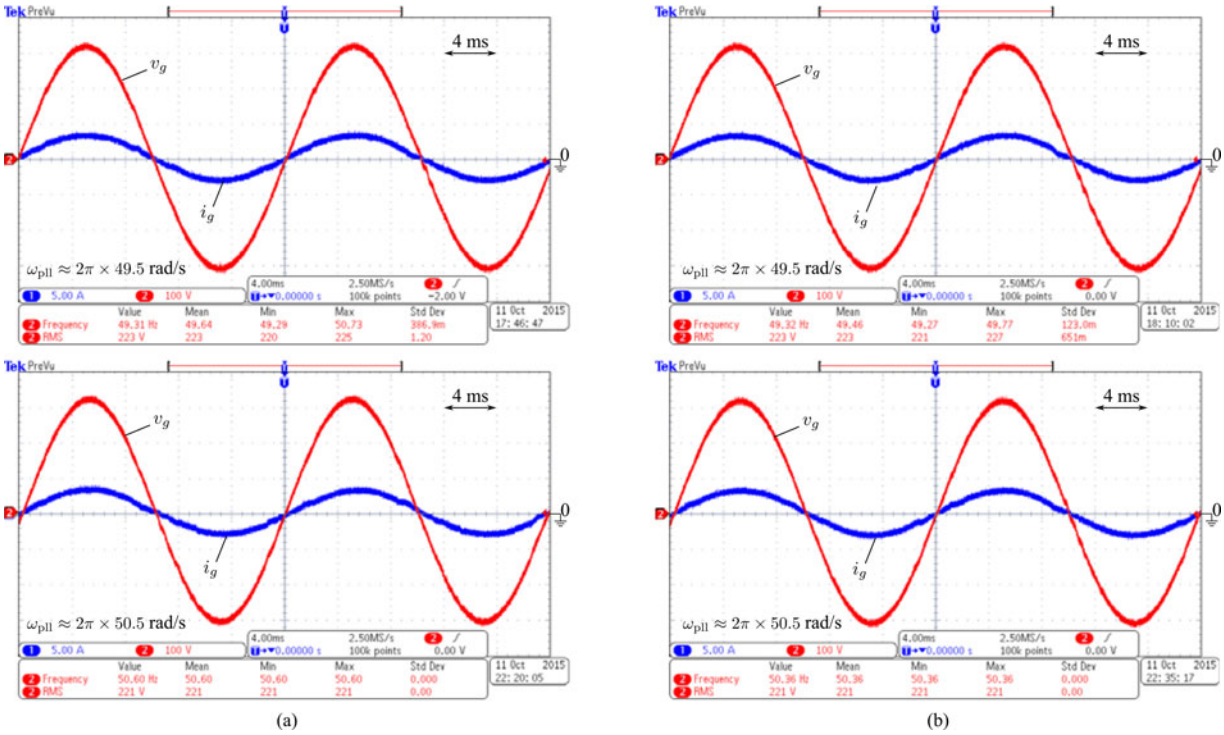


Fig. 17. Steady-state performance (half-loading, i.e., output power is 500 W) of the frequency adaptive PR controller in the case of abnormal grid frequencies with frequency adaptability enhanced harmonic compensators (CH1—grid current $i_g$ [5 A/div]; CH2—grid voltage $v_g$ [100 V/div]): (a) resonant controllers and (b) RC.

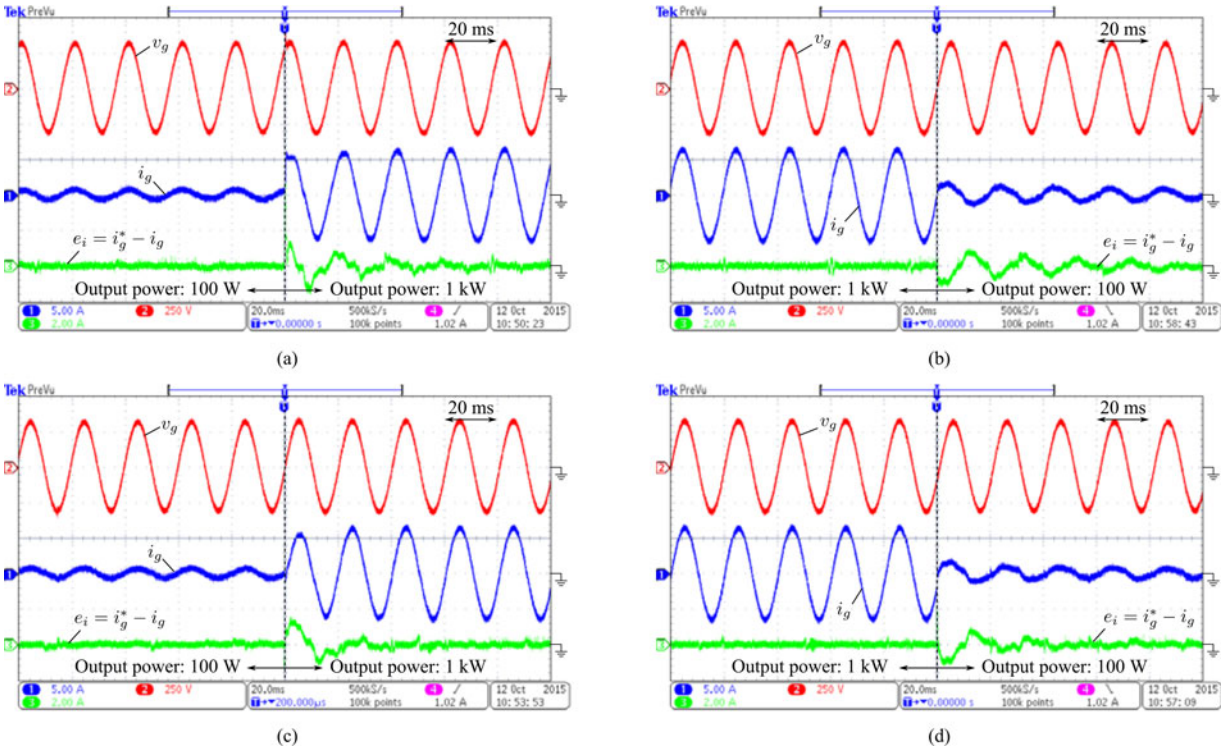


Fig. 18. Performance (loading transients) of the frequency adaptive PR controller with frequency adaptability enhanced harmonic compensators (CH1—grid current $i_g$ [5 A/div]; CH2—grid voltage $v_g$ [250 V/div]; CH3—current error $e_i = i_g^* - i_g$ [5 A/div]): (a) step-up load change from 100 W to 1 kW using RES harmonic compensator, (b) step-down load change from 1 kW to 100 W using RES harmonic compensator, (c) step-up load change from 100 W to 1 kW using RC harmonic compensator, and (d) step-down load change from 1 kW to 100 W using RC harmonic compensator, where the grid frequency is 49.5 Hz.

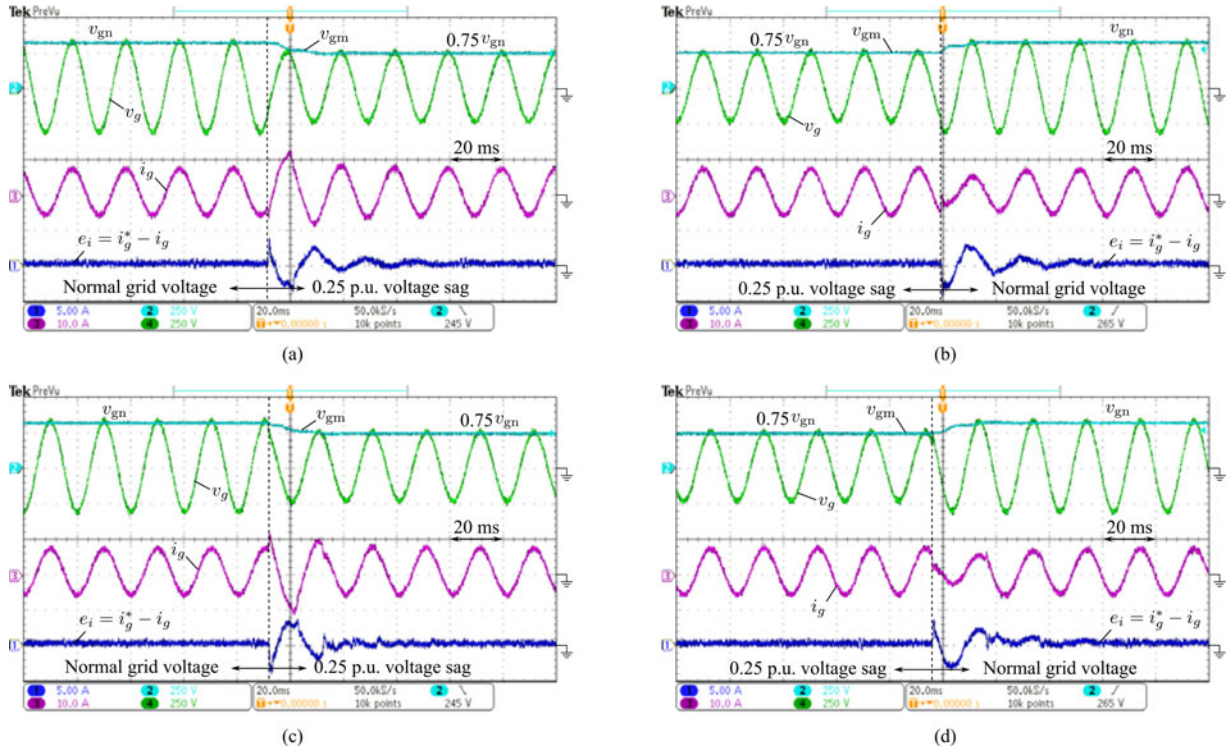


Fig. 19. Performance (voltage sag) of the frequency adaptive PR controller with frequency adaptability enhanced harmonic compensators (CH1—current error $e_i = i_g^* - i_g$ [5 A/div]; CH2—grid voltage amplitude (estimated by the PLL system) $v_{\rm gm}$ [250 V/div]; CH3—grid current $i_g$ [5 A/div]; CH4—grid voltage $v_g$ [250 V/div]): (a) in the case of a voltage drop by 0.25 p.u. using RES compensator, (b) during the grid voltage recovery using RES compensator, (c) in the case of a voltage drop by 0.25 p.u. using RC compensator, and (d) during the grid voltage recovery using RC compensator, where the grid frequency is 49.5 Hz.

grid-connected inverter system has been tested under various loading conditions. The $\text{THD}_{i_g}$ of the feed-in currents is plotted as shown in Fig. 16. The effectiveness of the frequency adaptive schemes can be identified in Fig. 16, where, for example, the $\text{THD}_{i_g}$ is reduced by around 0.5% and 1%, respectively, under abnormal grid conditions (i.e., the grid frequency is 49.5 or 50.5 Hz) in contrast to the results presented in Fig. 15(a) and (c). Fig. 17 presents the steady-state performance of the frequency adaptive current controllers under a half-loading condition, in which it can be observed that the unity power factor operation is always achieved despite of the abnormal grid frequencies. Those experimental tests have demonstrated that by feeding back the PLL estimated frequency to the RES controller and approximating the fractional delays for the RC compensator be means of Lagrange polynomial filters, the frequency adaptability of the corresponding periodic controller can be enhanced.

Moreover, robustness is another important index to assess the current controllers. Hence, the selected current controllers with enhanced frequency adaptability have been further tested in the case of loading transients. The performance of these periodic current controllers is given in Fig. 18, where the output power experienced a step-up change from 100 W to 1 kW and a step-down change from 1 kW to 100 W, and the grid frequency was programmed as 49.5 Hz. It can be seen in Fig. 18 that the frequency adaptive schemes for the RES controllers and the RC compensator have negligible influence on the dynamics of the entire current controller. Specifically, both frequency adaptive periodic current controllers can quickly come into the steady state without any compromise of stability. It should be noted that when the repetitive current controller is adopted as the harmonic compensator, the entire controller can achieve almost zero-error tracking of the grid current within three cycles. Additionally, seen from the experimental results in Figs. 17(b) and 18(c), (d), the frequency adaptive RC harmonic compensation has superior performance over the frequency adaptive RES-based harmonic compensator in terms of dynamics and harmonic mitigations, especially in light loading conditions.

Notably, the main idea behind the enhancement of the frequency adaptability in brief is to update the center frequency of the periodic current controllers according to the PLL estimated frequency. As a consequence, the response of the PLL system (i.e., the SOGI-PLL in this paper) to other abnormal grid conditions (e.g., grid voltage sags) may also affect the performance of the frequency adaptive current controllers. In order to validate the robustness of the selected periodic current controllers in the case of grid voltage sags, more experimental tests have been conducted on the single-phase system, where the grid frequency is 49.5 Hz and the grid current amplitude has been controlled as constant (i.e., $I_g^* = 6.43$ A, corresponding to the current at the rated power level) to avoid inverter shutdown due to overcurrent protection. The experimental results are presented in Fig. 19, where the grid voltage has sagged to 165 V in RMS (i.e., voltage sag level: 0.25 per unit (p.u.) during operation or reversely. It can be observed that the frequency adaptive current controllers by means of online updating the center frequency is robust even under grid voltage sags. In addition, the repetitive harmonic compensator has a faster response than the RES controller does, which is indicated by the current tracking errors ($e_i$)

in Fig. 19, and however, the dynamics are affected by the designed PLL systems. In this paper, the SOGI-PLL has relatively fast responses to abnormal grid conditions [8], and thus, it also contributes to the frequency adaptability of the selected periodic current controllers to some extent. Nevertheless, all the above experiments have demonstrated the frequency adaptability of the selected current controllers, and also the effectiveness of the frequency adaptive schemes for these periodic current controllers even under various grid disturbances (e.g., frequency changes and voltage sags).

## V. Conclusion

The sensitivity to frequency variations of selected current controllers for grid-connected power converters has been explored in this paper. The investigation has revealed that the DB current controller is almost immune to the frequency deviations, since it is a model-based predictive controller. In contrast, the PR controller, the RES harmonic compensator, and the RCs are very sensitive to the frequency variations induced by the PLL synchronization errors and/or the grid disturbances. This is because those periodic current controllers (harmonic compensators) are strongly dependent on the center frequencies, and infinite control gains at the frequencies of interest (e.g., the fundamental frequency) cannot be achieved due to the frequency deviations. In addition, this paper has also introduced means to enhance the frequency adaptability of the discussed current controllers—simply feeding back the PLL estimated frequency to the RES controller or properly approximating the fractional delay for the RC harmonic controller. Experiments performed on a single-phase grid-connected inverter have verified the discussions. It is worth pointing out that an advanced frequency estimator (e.g., a PLL synchronization system) in terms of relatively high accuracy in the estimated grid frequency and fast responses to grid disturbances is important for the periodic current controllers to ensure high-quality currents into the grid.

## References


[1] J. D. van Wyk and F. C. Lee, "On a future for power electronics," *IEEE J. Emerg. Sel. Topics Power Electron.*, vol. 1, no. 2, pp. 59–72, Jun. 2013.

[2] F. Blaabjerg, K. Ma, and Y. Yang, "Power electronics—The key technology for renewable energy systems," in *Proc. 9th Int. Conf. Ecological Veh. Renew. Energies*, Mar. 2014, pp. 1–11.

[3] Y. Yang, P. Enjeti, F. Blaabjerg, and H. Wang, "Wide-scale adoption of photovoltaic energy: Grid code modifications are explored in the distribution grid," *IEEE Ind. Appl. Mag.*, vol. 21, no. 5, pp. 21–31, Sep. 2015.

[4] A. Sangwongwanich, Y. Yang, and F. Blaabjerg, "High-performance constant power generation in grid-connected pv systems," *IEEE Trans. Power Electron.*, vol. 31, no. 3, pp. 1822–1825, Mar. 2016.

[5] International Electrotechnical Commission (IEC), *Characteristics of the Utility Interface for Photovoltaic Systems*, IEC Std 61727:2004, Dec. 2004.

[6] T. S. Basso, "IEEE 1547 and 2030 standards for distributed energy resources interconnection and interoperability with the electricity grid," Nat. Renewable Energy Lab., Golden, CO, USA, Tech. Rep. NREL/TP-5D00-63157, Dec. 2014.

[7] F. Blaabjerg, R. Teodorescu, M. Liserre, and A. V. Timbus, "Overview of control and grid synchronization for distributed power generation systems," *IEEE Trans. Ind. Electron.*, vol. 53, no. 5, pp. 1398–1409, Oct. 2006.

[8] M. Ciobotaru, R. Teodorescu, and F. Blaabjerg, "A new single-phase PLL structure based on second order generalized integrator," in *Proc. Power Electron. Spec. Conf.*, Jun. 2006, pp. 1–6.

[9] S. A. Khajehoddin, M. Karimi-Ghartemani, A. Bakhshai, and P. Jain, "A power control method with simple structure and fast dynamic response for single-phase grid-connected DG systems," *IEEE Trans. Power Electron.*, vol. 28, no. 1, pp. 221–233, Jan. 2013.

[10] R. M. Santos Filho, P. F. Seixas, P. C. Cortizo, L. A. B. Torres, and A. F. Souza, "Comparison of three single-phase PLL algorithms for UPS applications," *IEEE Trans. Ind. Electron.*, vol. 55, no. 8, pp. 2923–2932, Aug. 2008.

[11] S. Golestan, M. Monfared, F. D. Freijedo, and J. M. Guerrero, "Design and tuning of a modified power-based PLL for single-phase grid-connected power conditioning systems," *IEEE Trans. Power Electron.*, vol. 27, no. 8, pp. 3639–3650, Aug. 2012.

[12] Y. Han, M. Luo, X. Zhao, J. Guerrero, and L. Xu, "Comparative performance evaluation of orthogonal-signal-generators based single-phase PLL algorithms—A survey," *IEEE Trans. Power Electron.*, vol. 31, no. 5, pp. 3932–3944, May 2016.

[13] P. Roncero-Sanchez, X. del Toro Garcia, A. P. Torres, and V. Feliu, "Robust frequency-estimation method for distorted and imbalanced three-phase systems using discrete filters," *IEEE Trans. Power Electron.*, vol. 26, no. 4, pp. 1089–1101, Apr. 2011.

[14] Md. S. Reza, M. Ciobotaru, and V. G. Agelidis, "Single-phase grid voltage frequency estimation using teager energy operator based technique," *IEEE J. Emerg. Sel. Topics Power Electron.*, vol. 3, no. 4, pp. 1218–1227, Dec. 2015.

[15] L. Hadjidemetriou, E. Kyriakides, Y. Yang, and F. Blaabjerg, "A synchronization method for single-phase grid-tied inverters," *IEEE Trans. Power Electron.*, vol. 31, no. 3, pp. 2139–2149, Mar. 2016.

[16] R. Teodorescu, M. Liserre, and P. Rodriguez, *Grid Converters for Photovoltaic and Wind Power Systems*. Piscataway, NJ, USA: IEEE Press, 2011.

[17] M. Ebrahimi, S. Khajehoddin, and M. Karimi Ghartemani, "Fast and robust single-phase dq current controller for smart inverter applications," *IEEE Trans. Power Electron.*, vol. 31, no. 5, pp. 3968–3976, May 2016.

[18] Y. Yang and F. Blaabjerg, "Overview of single-phase grid-connected photovoltaic systems," *Electr. Power Compon. Syst.*, vol. 43, no. 12, pp. 1352–1363, 2015.

[19] Y. Song and H. Nian, "Sinusoidal output current implementation of DFIG using repetitive control under generalized harmonic power grid with frequency deviation," *IEEE Trans. Power Electron.*, vol. 30, no. 12, pp. 6751–6762, Dec. 2015.

[20] Y. Yang, K. Zhou, H. Wang, F. Blaabjerg, D. Wang, and B. Zhang, "Frequency adaptive selective harmonic control for grid-connected inverters," *IEEE Trans. Power Electron.*, vol. 30, no. 7, pp. 3912–3924, Jul. 2015.

[21] M. A. Herran, J. R. Fischer, S. A. Gonzalez, M. G. Judewicz, I. Carugati, and D. O. Carrica, "Repetitive control with adaptive sampling frequency for wind power generation systems," *IEEE J. Emerg. Sel. Topics Power Electron.*, vol. 2, no. 1, pp. 58–69, Mar. 2014.

[22] M. Rashed, C. Klumpner, and G. Asher, "Repetitive and resonant control for a single-phase grid-connected hybrid cascaded multilevel converter," *IEEE Trans. Power Electron.*, vol. 28, no. 5, pp. 2224–2234, May 2013.

[23] A. Garcia-Cerrada, O. Pinzon-Ardila, V. Feliu-Batlle, P. Roncero-Sanchez, and P. Garcia-Gonzalez, "Application of a repetitive controller for a three-phase active power filter," *IEEE Trans. Power Electron.*, vol. 22, no. 1, pp. 237–246, Jan. 2007.

[24] A. Lidozzi, C. Ji, L. Solero, P. Zanchetta, and F. Crescimbini, "Resonant-repetitive combined control for stand-alone power supply units," *IEEE Trans. Ind. Appl.*, vol. 51, no. 6, pp. 4653–4663, Nov./Dec. 2015.

[25] T. Liu, D. Wang, and K. Zhou, "High-performance grid simulator using parallel structure fractional repetitive control," *IEEE Trans. Power Electron.*, vol. 31, no. 3, pp. 2669–2679, Mar. 2016.

[26] S. A. Khajehoddin, M. Karimi-Ghartemani, P. K. Jain, and A. Bakhshai, "A resonant controller with high structural robustness for fixed-point digital implementations," *IEEE Trans. Power Electron.*, vol. 27, no. 7, pp. 3352–3362, Jul. 2012.

[27] M. Liserre, R. Teodorescu, and F. Blaabjerg, "Multiple harmonics control for three-phase grid converter systems with the use of PI-RES current controller in a rotating frame," *IEEE Trans. Power Electron.*, vol. 21, no. 3, pp. 836–841, May 2006.

[28] A. G. Yepes, F. D. Freijedo, O. Lopez, and J. Doval-Gandoy, "High-performance digital resonant controllers implemented with two integrators," *IEEE Trans. Power Electron.*, vol. 26, no. 2, pp. 563–576, Feb. 2011.

[29] F. González-Espín, G. Garcerá, I. Patrao, and E. Figueres, "An adaptive control system for three-phase photovoltaic inverters working in a polluted and variable frequency electric grid," *IEEE Trans. Power Electron.*, vol. 27, no. 10, pp. 4248–4261, Oct. 2012.

[30] D. J. Hogan, F. Gonzalez-Espin, J. G. Hayes, G. Lightbody, and M. G. Egan, "Adaptive resonant current-control for active power filtering within a microgrid," in *Proc. Energy Convers. Congr. Expo.*, Sep. 2014, pp. 3468–3475.
[31] M. Mascioli, M. Pahlevani, and P. Jain, "Frequency-adaptive current controller for grid-connected renewable energy systems," in *Proc. 36th Int. Telecommun. Energy Conf.*, Sep. 2014, pp. 1–6.
[32] S. Gomez Jorge, C. A. Busada, and J. A. Solsona, "Frequency-adaptive current controller for three-phase grid-connected converters," *IEEE Trans. Ind. Electron.*, vol. 60, no. 10, pp. 4169–4177, Oct. 2013.
[33] Y. Yang, K. Zhou, and F. Blaabjerg, "Frequency adaptability of harmonics controllers for grid-interfaced converters," *Int. J. Control*, pp. 1–12, 2015, DOI: 10.1080/00207179.2015.1022957.
[34] J. Kim, K. Chang, I. Shim, G. Park, and S. Kim, "Corrections to 'adaptive repetitive control for an eccentricity compensation of optical disk drivers'," *IEEE Trans. Consumer Electron.*, vol. 53, no. 3, pp. 962–968, Aug. 2007.
[35] F. D. Freijedo, A. G. Yepes, J. Malvar, O. Lopez, P. Fernandez-Comesana, A. Vidal, and J. Doval-Gandoy, "Frequency tracking of digital resonant filters for control of power converters connected to public distribution systems," *IET Power Electron.*, vol. 4, no. 4, pp. 454–462, 2011.
[36] D. Chen, J. Zhang, and Z. Qian, "An improved repetitive control scheme for grid-connected inverter with frequency-adaptive capability," *IEEE Trans. Ind. Electron.*, vol. 60, no. 2, pp. 814–823, Feb. 2013.
[37] G. Escobar, M. Hernandez-Gomez, A. A. Valdez-Fernandez, M. J. Lopez-Sanchez, and G. A. Catzin-Contreras, "Implementation of a $6n \pm 1$ repetitive controller subject to fractional delays," *IEEE Trans. Ind. Electron.*, vol. 62, no. 1, pp. 444–452, Jan. 2015.
[38] M. Abusara, S. Sharkh, and P. Zanchetta, "Adaptive repetitive control with feedforward scheme for grid-connected inverters," *IET Power Electron.*, vol. 8, no. 8, pp. 1403–1410, Aug. 2015.
[39] J. M. Olm, G. A. Ramos, and R. Costa-Castello, "Stability analysis of digital repetitive control systems under time-varying sampling period," *IET Control Theory Appl.*, vol. 5, no. 1, pp. 29–37, Jan. 2011.
[40] Z. Cao and G. F. Ledwich, "Adaptive repetitive control to track variable periodic signals with fixed sampling rate," *IEEE/ASME Trans. Mechatron.*, vol. 7, no. 3, pp. 378–384, Sep. 2002.
[41] B. Zhang, K. Zhou, and D. Wang, "Multirate repetitive control for PWM DC/AC converters," *IEEE Trans. Ind. Electron.*, vol. 61, no. 6, pp. 2883–2890, Jun. 2014.
[42] Z. Zou, K. Zhou, Z. Wang, and M. Cheng, "Fractional-order repetitive control of programmable AC power sources," *IET Power Electron.*, vol. 7, no. 2, pp. 431–438, Feb. 2014.
[43] J. C. Boemer, K. Burges, P. Zolotarev, J. Lehner, P. Wajant, M. Fürst, R. Brohm, and T. Kumm, "Overview of German grid issues and retrofit of photovoltaic power plants in German for the prevention of frequency stability problems in abnormal system conditions of the ENTSO-E region continental Europe," presented at the 1st Solar Int. Workshop, Aarhus, Denmark, Oct. 2011, vol. 24.
[44] T. Ackermann, A. Ellis, J. Fortmann, J. Matevosyan, E. Muljadi, R. Piwko, P. Pourbeik, E. Quitmann, P. Sorensen, H. Urdal, and B. Zavadil, "Code shift: Grid specifications and dynamic wind turbine models," *IEEE Power Energy Mag.*, vol. 11, no. 6, pp. 72–82, Nov. 2013.
[45] M. Tsili and S. Papathanassiou, "A review of grid code technical requirements for wind farms," *IET Renew. Power Gener.*, vol. 3, no. 3, pp. 308–332, Sep. 2009.
[46] K. Nishida, T. Ahmed, and M. Nakaoka, "Cost-effective deadbeat current control for wind-energy inverter application with LCL filter," *IEEE Trans. Ind. Appl.*, vol. 50, no. 2, pp. 1185–1197, Mar./Apr. 2014.
[47] K. Zhou, Y. Yang, F. Blaabjerg, and D. Wang, "Optimal selective harmonic control for power harmonics mitigation," *IEEE Trans. Ind. Electron.*, vol. 62, no. 2, pp. 1220–1230, Feb. 2015.
[48] R. Costa-Castello, J. Nebot, and R. Grino, "Demonstration of the internal model principle by digital repetitive control of an educational laboratory plant," *IEEE Trans. Edu.*, vol. 48, no. 1, pp. 73–80, Feb. 2005.
[49] M. Zamani, N. Wrathall, and R. Beresh, "A review of the latest voltage and frequency ride-through requirements in Canadian jurisdictions," in *Proc. IEEE Electr. Power Energy Conf.*, Nov. 2014, pp. 116–121.
[50] T. I. Laakso, V. Valimaki, M. Karjalainen, and U. K. Laine, "Splitting the unit delay—FIR/all pass filters design," *IEEE Signal Process. Mag.*, vol. 13, no. 1, pp. 30–60, Jan. 1996.
[51] Y. He, H. Chung, C. Ho, and W. Wu, "Use of boundary control with second-order switching surface to reduce the system order for deadbeat controller in grid-connected inverter," *IEEE Trans. Power Electron.*, vol. 31, no. 3, pp. 2638–2653, Mar. 2016.
[52] Y. Yang, K. Zhou, and F. Blaabjerg, "Current harmonics from single-phase grid-connected inverters—Examination and suppression," *IEEE J. Emerg. Sel. Topics Power Electron.*, 2016, to be published, DOI: 10.1109/JESTPE.2015.2504845.
[53] D. Dong, B. Wen, D. Boroyevich, P. Mattavelli, and Y. Xue, "Analysis of phase-locked loop low-frequency stability in three-phase grid-connected power converters considering impedance interactions," *IEEE Trans. Ind. Electron.*, vol. 62, no. 1, pp. 310–321, Jan. 2015.

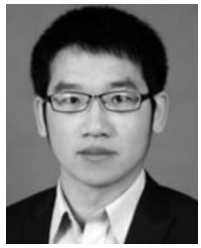

**Yongheng Yang** (S'12–M'15) received the B.Eng. degree from Northwestern Polytechnical University, Xian, China, in 2009, and the Ph.D. degree from Aalborg University, Aalborg, Denmark, in 2014.

He was a Postgraduate with Southeast University, Nanjing, China, from 2009 to 2011. In 2013, he was a Visiting Scholar with the Department of Electrical and Computer Engineering, Texas A&M University, College Station, TX, USA. Since 2014, he has been with the Department of Energy Technology, Aalborg University, where he is currently an Assistant Professor. His research interests include grid integration and control of renewable energy systems, harmonics in adjustable speed drives and grid-connected power converters, and the reliability of power electronics.

Dr. Yang is involved in the IEEE Industry Applications Society student activities. He is a Committee Member of the IEEE Power Electronics Society Young Professionals and responsible for the webinar series. He serves as a Guest Associate Editor of the IEEE JOURNAL OF EMERGING AND SELECTED TOPICS IN POWER ELECTRONICS special issue on Power Electronics for Energy Efficient Buildings, and a Session Chair for various technical conferences.

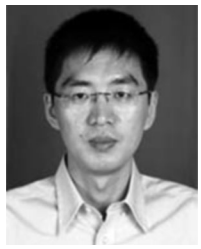

**Keliang Zhou** (M'04–SM'08) received the B.Sc. degree from the Huazhong University of Science and Technology, Wuhan, China, the M.Eng. degree from Wuhan Transportation University (now the Wuhan University of Technology), Wuhan, and the Ph.D. degree from Nanyang Technological University, Singapore, in 1992, 1995, and 2002, respectively.

During 2003–2006, he was a Research Fellow with Nanyang Technological University in Singapore and with the Delft University of Technology, Delft, the Netherlands, respectively. From 2006 to 2014, he was with Southeast University in China and with the University of Canterbury in New Zealand, respectively. As a Senior Lecturer, he joined the School of Engineering at the University of Glasgow, Glasgow, U.K., in 2014. He has authored or coauthored more than 100 technical papers and several granted patents in relevant areas. His teaching and research interests include power electronics and electric drives, renewable energy generation, control theory and applications, and microgrid technology.

**Frede Blaabjerg** (S'86–M'88–SM'97–F'03) was with ABB-Scandia, Randers, Denmark, from 1987 to 1988. He received the Ph.D. degree from Aalborg University, Aalborg, Denmark, in 1992.

He became an Assistant Professor in 1992, an Associate Professor in 1996, and a Full Professor of power electronics and drives in 1998, with Aalborg University. His current research interests include power electronics and its applications such as in wind turbines, photovoltaic systems, reliability, harmonics and adjustable speed drives.

Prof. Blaabjerg received 15 IEEE Prize Paper Awards, the IEEE PELS Distinguished Service Award in 2009, the EPE-PEMC Council Award in 2010, the IEEE William E. Newell Power Electronics Award 2014, and the Villum Kann Rasmussen Research Award 2014. He was an Editor-in-Chief of the IEEE TRANSACTIONS ON POWER ELECTRONICS from 2006 to 2012. He has been a Distinguished Lecturer for the IEEE Power Electronics Society from 2005 to 2007 and for the IEEE Industry Applications Society from 2010 to 2011. He is nominated by Thomson Reuters in 2014 to be between the most 250 cited researchers in Engineering in the world.